SUPERCONDUCTIVITY

OVERVIEW OF EXPERIMENTAL FACTS
EARLY MODELS
GINZBURG-LANDAU THEORY
BCS THEORY

Jean Delayen

Thomas Jefferson National Accelerator Facility
Old Dominion University

Historical Overview

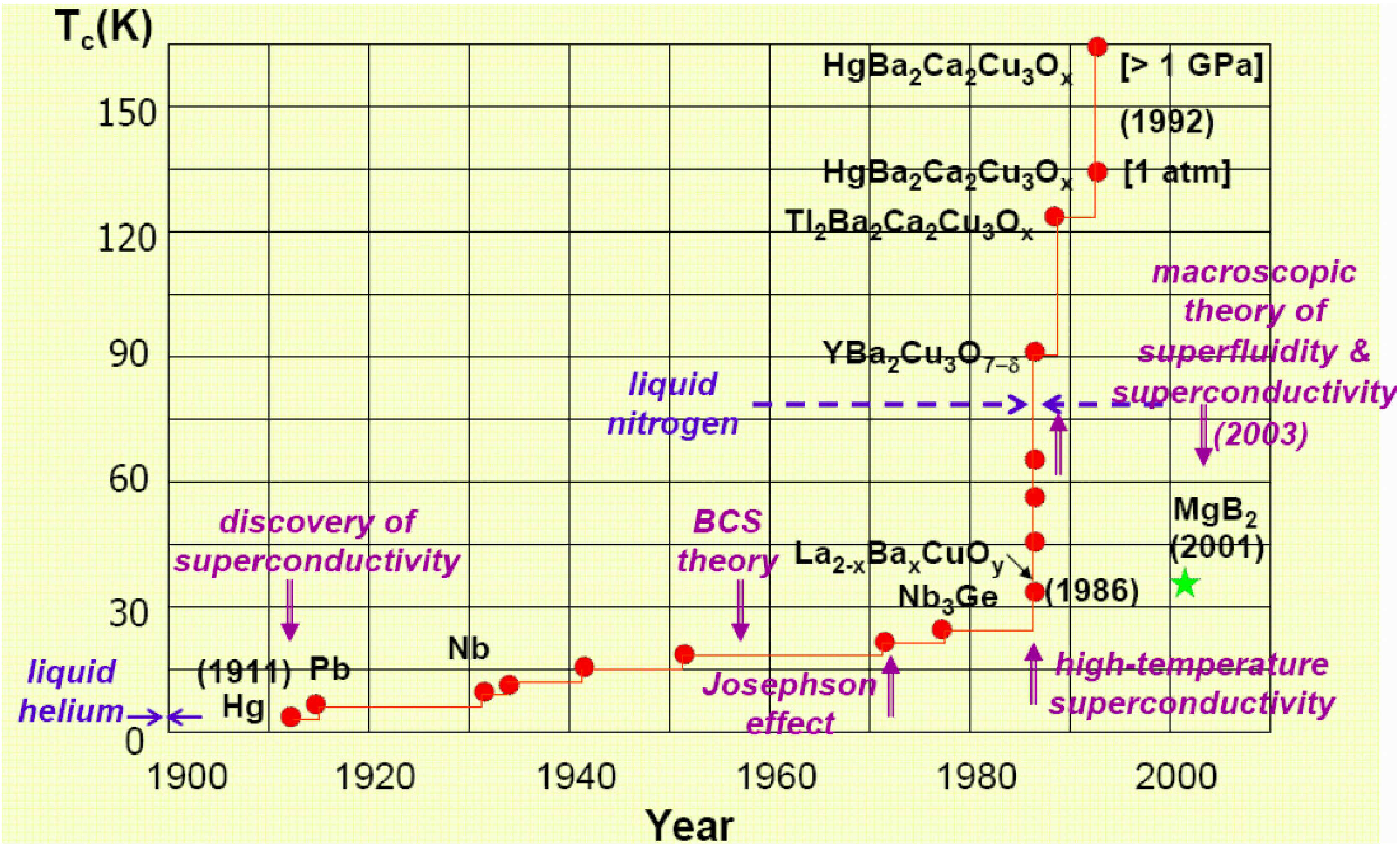

Perfect Conductivity

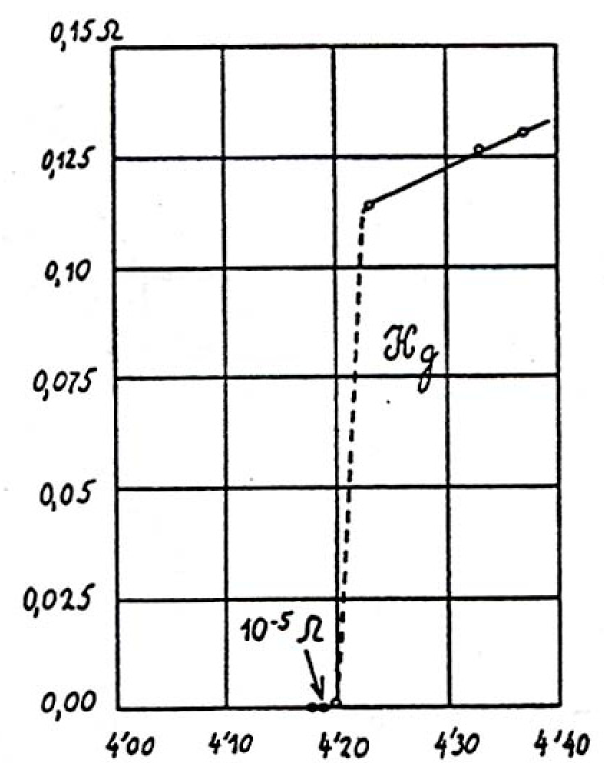

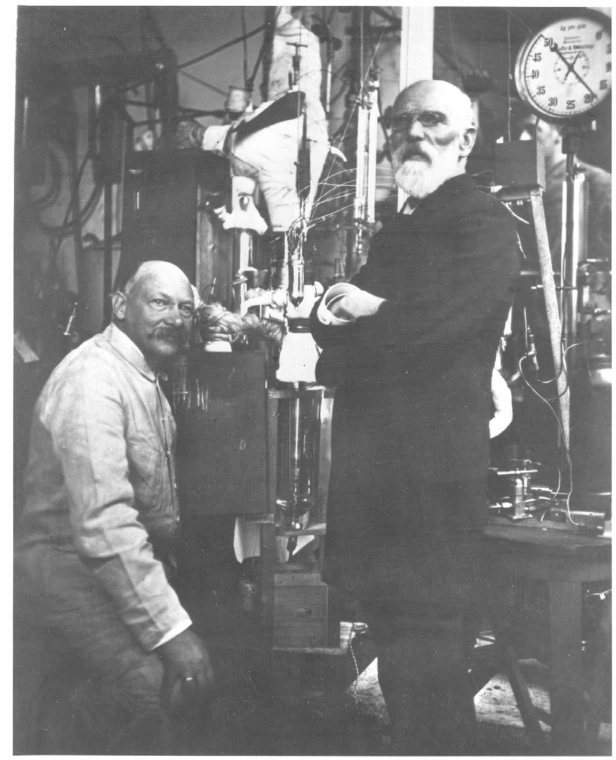

Kamerlingh Onnes and van der Waals in Leiden with the helium 'liquefactor' (1908)

Unexpected result

Expectation was the opposite: everything should become an isolator at $T \to 0$

Perfect Conductivity

Persistent current experiments on rings have measured

$$\frac{\sigma_s}{\sigma_n} > 10^{15}$$

Resistivity < 10^{-23} Ω.cm

Decay time > 10^5 years

Perfect conductivity is not superconductivity

Superconductivity is a phase transition

A perfect conductor has an infinite relaxation time L/R

Perfect Diamagnetism (Meissner & Ochsenfeld 1933)

Perfect conductor

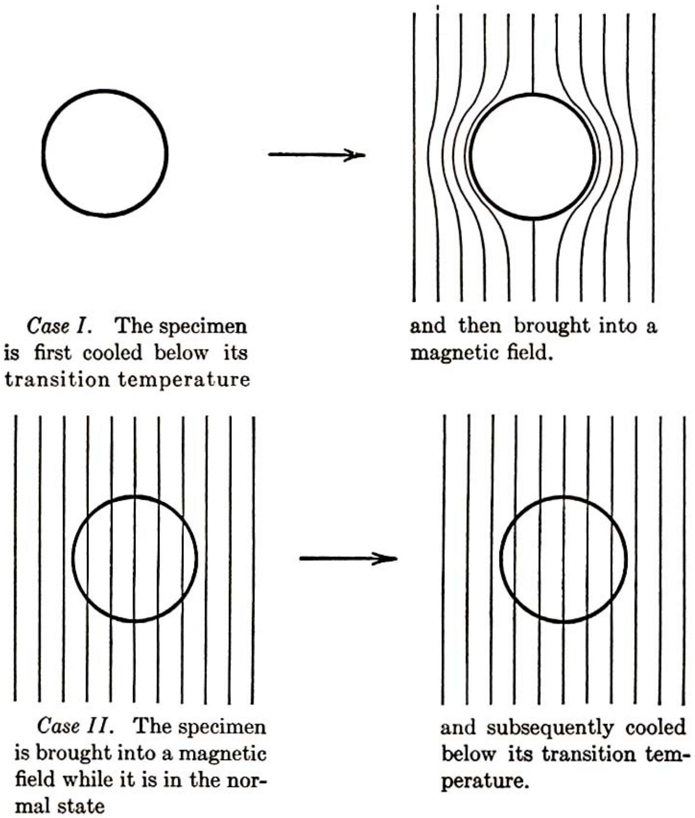

FIG. 3. The behavior expected for a transition into a state of *perfect conductivity.* The final state would depend on the *serial order* in which the specimen is brought into the same external conditions.

$$\frac{\partial B}{\partial t} = 0$$

Superconductor

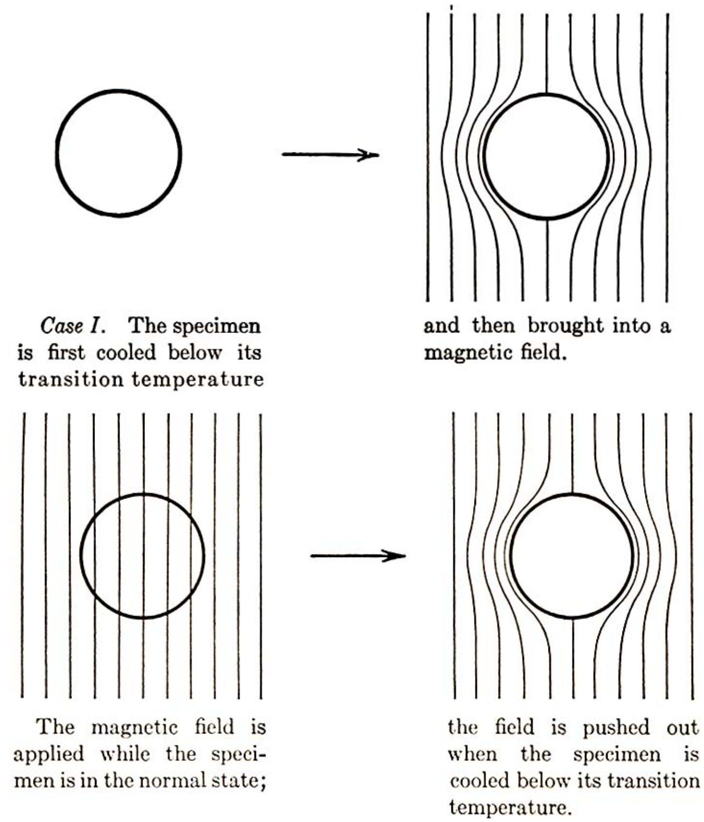

FIG. 4. Case II of Fig. 3 according to Meissner. The *superconductor*, in contrast to the perfect conductor, has zero magnetic induction independently of the way in which the superconducting state has been reached.

$$B = 0$$

Penetration Depth in Thin Films

Very thin films

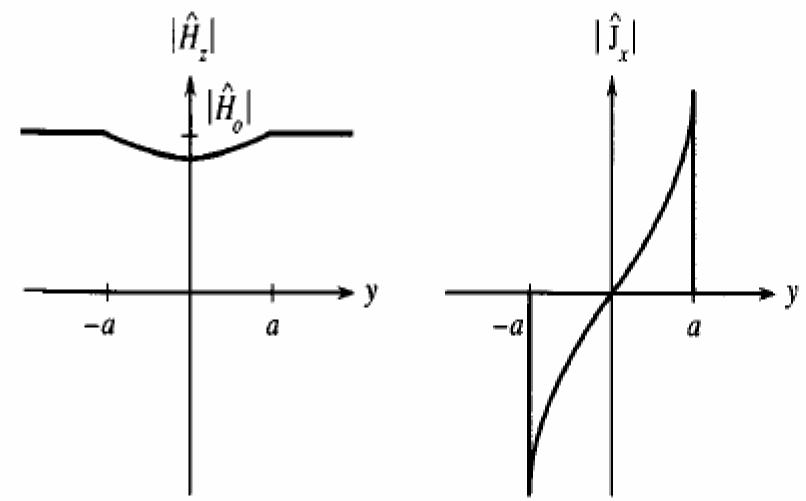

Very thick films

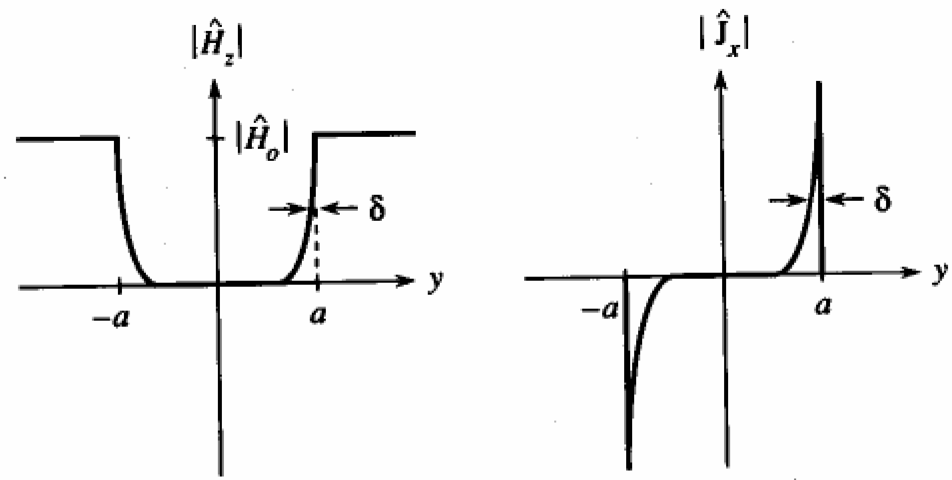

Critical Field (Type I)

Superconductivity is destroyed by the application of a magnetic field

$$H_c(T) \simeq H_c(0)\left[1-\left(\frac{T}{T_c}\right)^2\right]$$

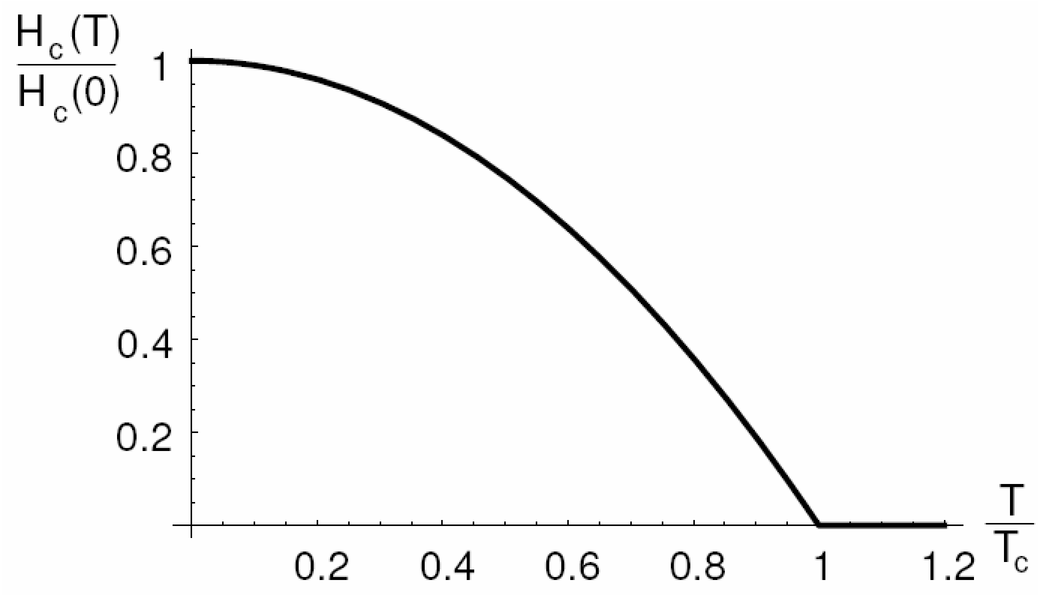

Type I or “soft” superconductors

Critical Field (Type II or "hard" superconductors)

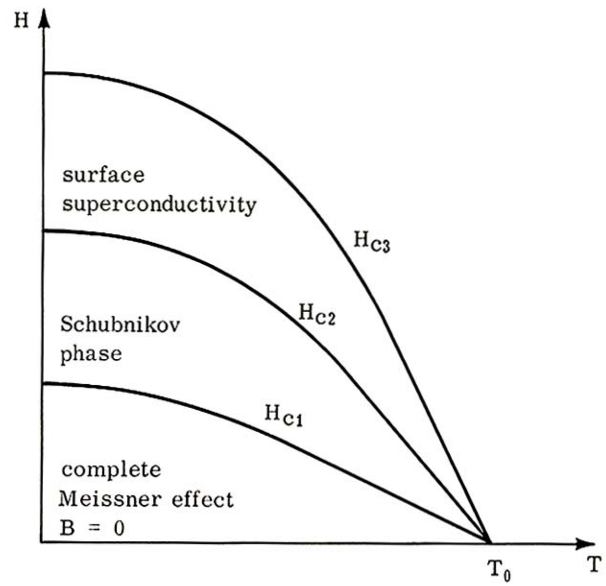

Figure 3-1
Phase diagram for a long cylinder of a Type II superconductor.

Expulsion of the magnetic field is complete up to H_{c1}, and partial up to H_{c2}

Between H_{c1} and H_{c2} the field penetrates in the form if quantized vortices or fluxoids

$$\phi_0 = \frac{\pi\hbar}{e}$$

Thermodynamic Properties

Entropy

Specific Heat

Energy

Free Energy

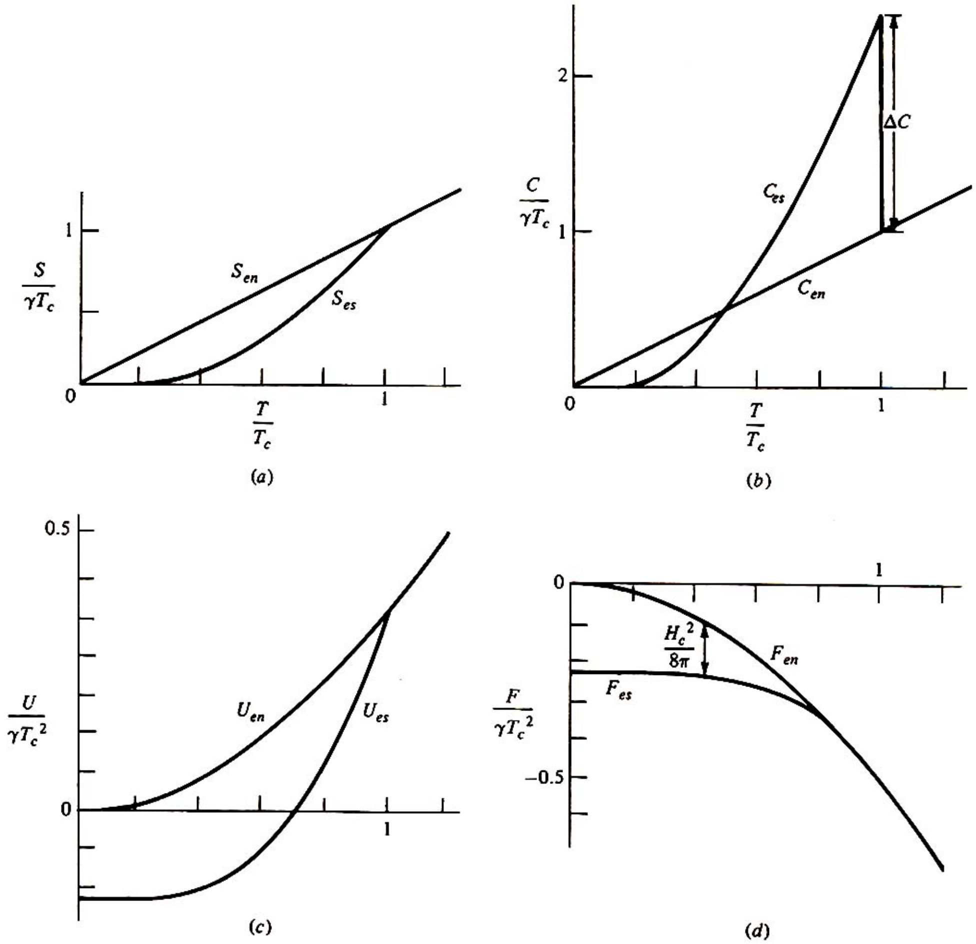

FIGURE 2-3
Comparison of thermodynamic quantities in superconducting and normal states. $U_{en}(0)$ is chosen as the zero of ordinates in (c) and (d). Because the transition is of second order, the quantities S, U, and F are continuous at T_c. Moreover, the slope of F_{es} joins continuously to that of F_{en} at T_c, since $\partial F/\partial T = -S$.

Thermodynamic Properties

When $T < T_c$ phase transition at $H = H_c(T)$ is of 1st order $\longrightarrow$ latent heat

At $T = T_c$, phase transition is of 2nd order

no latent heat

jump in heat capacity

$$C_{es}(T_c) \sim 3C_{en}(T_c)$$

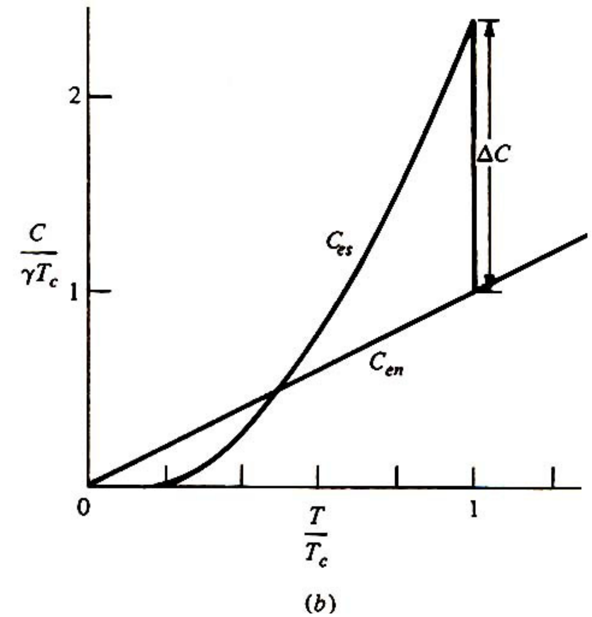

$C_{en} = \gamma T$ (electronic specific heat)

$C_{es} \approx \alpha T^3$ (reasonable fit to experimental data)

Thermodynamic Properties

At T_c : $S_s(T_c) = S_n(T_c)$ The entropy is continuous

Recall: $S(0) = 0$ and $\frac{\partial S}{\partial T} = \frac{C}{T}$

$$\Rightarrow \int_0^{T_c} \frac{\alpha T^3}{T} dt = \int_0^{T_c} \frac{\gamma T}{T} dt \to \alpha = \frac{3\gamma}{T_c^2} \qquad C_{es} = 3\gamma \frac{T^3}{T_c^2}$$

$$S_s(T) = \gamma \frac{T^3}{T_c^3} \qquad S_n(T) = \gamma \frac{T}{T_c}$$

For $T < T_c$ $S_s(T) < S_n(T)$

$\Rightarrow$ **superconducting state is more ordered than normal state**

A better fit for the electron specific heat in superconducting state is

$$C_{es} = a\gamma T_c\, e^{-\frac{bT_c}{T}} \text{ with } a \approx 9, b \approx 1.5 \text{ for } T \ll T_c$$

Energy Difference Between Normal and Superconducting State

$$U_n(T_c) = U_s(T_c)$$ Energy is continuous

$$U_n(T) - U_s(T) = \int_T^{T_c} (C_{es} - C_{en}) dt = \frac{3}{4}\frac{\gamma}{T_c^2}(T_c^4 - T^4) - \frac{\gamma}{2}\left(T_c^2 - T^2\right)$$

at $T=0$ $\quad U_n(0) - U_s(0) = \frac{1}{4}\gamma T_c^2 = \frac{H_c^2}{8\pi}$ $\qquad \frac{H_c^2}{8\pi}$ is the condensation energy

at $T \neq 0,$ $\frac{H_c^2}{8\pi}$ is the free energy difference

$$\frac{H_c^2(T)}{8\pi} = \Delta F = \left(U_n - U_s\right) - T\left(S_n - S_c\right) = \frac{1}{4}\gamma T_c^2\left[1 - \left(\frac{T}{T_c}\right)^2\right]^2$$

$$H_c(T) = (2\pi\gamma)^{\frac{1}{2}} T_c\left[1 - \left(\frac{T}{T_c}\right)^2\right]$$

The quadratic dependence of critical field on T is related to the cubic dependence of specific heat

Isotope Effect (Maxwell 1950)

The critical temperature and the critical field at 0K are dependent on the mass of the isotope

$$T_c \sim H_c(0) \sim M^{-\alpha} \qquad \text{with } \alpha \simeq 0.5$$

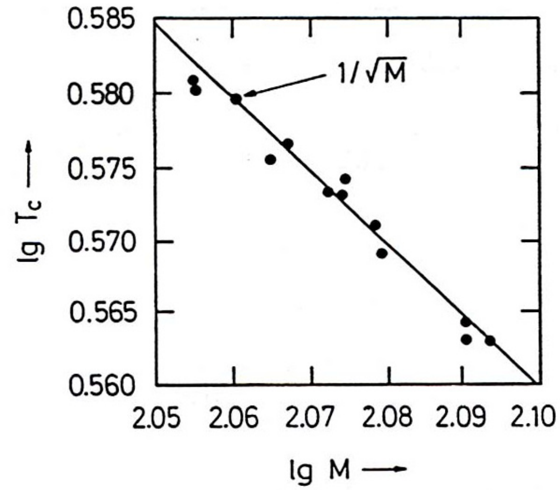

Figure 26: The critical temperature of various tin isotopes.

Energy Gap (1950s)

At very low temperature the specific heat exhibits an exponential behavior

$$c_s \propto e^{-bT_c/T} \qquad \text{with } b \simeq 1.5$$

Electromagnetic absorption shows a threshold

Tunneling between 2 superconductors separated by a thin oxide film shows the presence of a gap

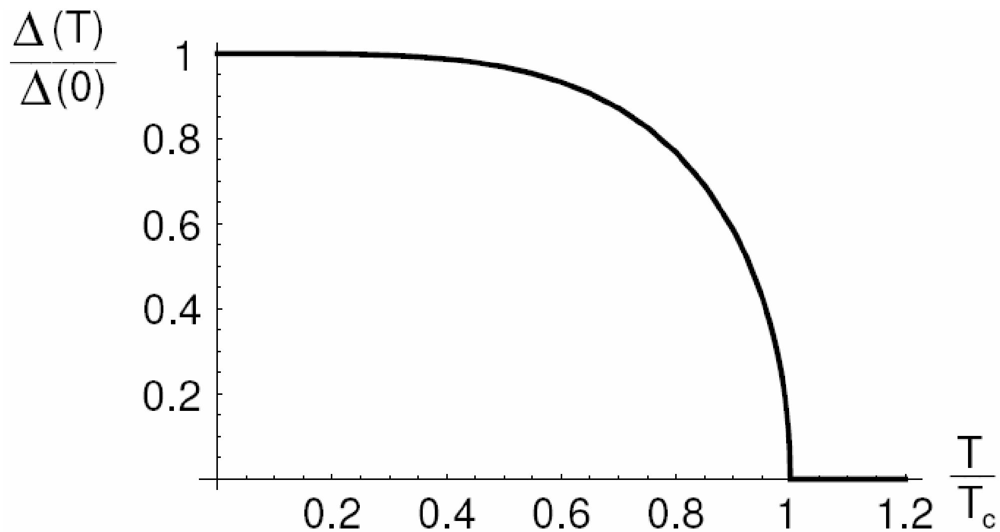

Two Fundamental Lengths

- London penetration depth λ
  - Distance over which magnetic fields decay in superconductors
- Pippard coherence length ξ
  - Distance over which the superconducting state decays

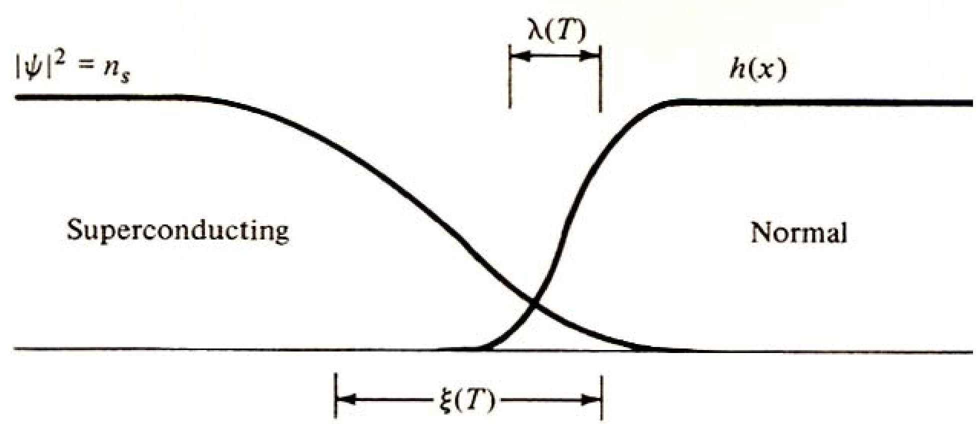

FIGURE 1-4
Interface between superconducting and normal domains in the intermediate stc

Two Types of Superconductors

- London superconductors (Type II)
  - $\lambda \gg \xi$
  - Impure metals
  - Alloys
  - Local electrodynamics

- Pippard superconductors (Type I)
  - $\xi \gg \lambda$
  - Pure metals
  - Nonlocal electrodynamics

Material Parameters for Some Superconductors

Superconductor	λ_L (0) (nm)	ξ_0 (nm)	κ	$2\Delta(0)/kT_c$	T_c(K)
Al	16	1500	0.011	3.40	1.18
In	25	400	0.062	3.50	3.3
Sn	28	300	0.093	3.55	3.7
Pb	28	110	0.255	4.10	7.2
Nb	32	39	0.82	3.5-3.85	8.95-9.2
Ta	35	93	0.38	3.55	4.46
Nb_3Sn	50	6	8.3	4.4	18
NbN	50	6	8.3	4.3	≤ 17
$Yba_2Cu_3o_x$	140	1.5	93	4.5	90

Phenomenological Models (1930s to 1950s)

Phenomenological model:

Purely descriptive

Everything behaves as though…..

A finite fraction of the electrons form some kind of condensate that behaves as a macroscopic system (similar to superfluidity)

At 0K, condensation is complete

At T_c the condensate disappears

Two Fluid Model – Gorter and Casimir

$T < T_c$ $\quad x =$ fraction of "normal" electrons

$(1 - x)$: fraction of "condensed" electrons (zero entropy)

Assume: $\quad F(T) = x^{1/2} f_n(T) + (1-x) f_s(T)$ $\quad$ free energy

$$f_n(T) = -\frac{1}{2}\gamma T^2$$

$$f_s(T) = -\beta = -\frac{1}{4}\gamma T_c^2$$ independent of temperature

Minimization of $F(T)$ gives $\quad x = \left(\frac{T}{T_C}\right)^4$

$$\Rightarrow F(T) = x^{1/2} f_n(T) + (1-x) f_s(T) = -\beta\left[1 + \left(\frac{T}{T_C}\right)^4\right]$$

$$\Rightarrow C_{es} = 3\gamma \frac{\mathrm{T}^3}{\mathrm{T}_\mathrm{C}^2}$$

Two Fluid Model – Gorter and Casimir

Superconducting state: $$F(T) = x^{1/2} f_n(T) + (1-x) f_s(T) = -\beta\left[1 + \left(\frac{T}{T_C}\right)^4\right]$$

Normal state: $$F(T) = f_n(T) = -\frac{\gamma}{2}T^2 = -2\beta\left(\frac{T}{T_C}\right)^2$$

Recall $\dfrac{H_c^2}{8\pi} =$ difference in free energy between normal and superconducting state

$$= \beta\left[1 - \left(\frac{T}{T_C}\right)^2\right]^2$$

$$\Rightarrow \quad \frac{H_c(T)}{H_c(0)} = 1 - \left(\frac{T}{T_C}\right)^2$$

The Gorter-Casimir model is an “ad hoc” model (there is no physical basis for the assumed expression for the free energy) but provides a fairly accurate representation of experimental results

Model of F & H London (1935)

Proposed a 2-fluid model with a normal fluid and superfluid components

n_s : density of the superfluid component of velocity $\mathbf{v}_s$
n_n : density of the normal component of velocity $\mathbf{v}_n$

$$m\frac{\partial \vec{v}}{\partial t} = -e\vec{E}$$ superelectrons are accelerated by E

$$\overrightarrow{J_s} = -en_s\ \vec{v}$$

$$\frac{\partial \vec{J}_s}{\partial t} = \frac{n_s e^2}{m}\vec{E}$$ superelectrons

$$\vec{J}_n = \sigma_n \vec{E}$$ normal electrons

Model of F & H London (1935)

$$\frac{\partial \vec{J}_s}{\partial t} = \frac{n_s e^2}{m}\vec{E}$$

Maxwell: $$\vec{\nabla} \times \vec{E} = -\frac{\partial \vec{B}}{\partial t}$$

$$\Rightarrow \frac{\partial}{\partial t}\left(\frac{m}{n_s e^2}\vec{\nabla} \times \vec{J}_s + \vec{B}\right) = 0 \qquad \Rightarrow \frac{m}{n_s e^2}\vec{\nabla} \times \vec{J}_s + \vec{B} = \text{Constant}$$

F&H London postulated: $$\boxed{\frac{m}{n_s e^2}\vec{\nabla} \times \vec{J}_s + \vec{B} = 0}$$

Model of F & H London (1935)

combine with $\vec{\nabla} \times \vec{B} = \mu_o \vec{J}_s$

$$\boxed{\nabla^2 \vec{B} - \frac{\mu_0 n_s e^2}{m} \vec{B} = 0}$$

$$B(x) = B_0 \exp\left[-x / \lambda_L\right]$$

$$\lambda_L = \left[\frac{m}{\mu_0 n_s e^2}\right]^{\frac{1}{2}}$$

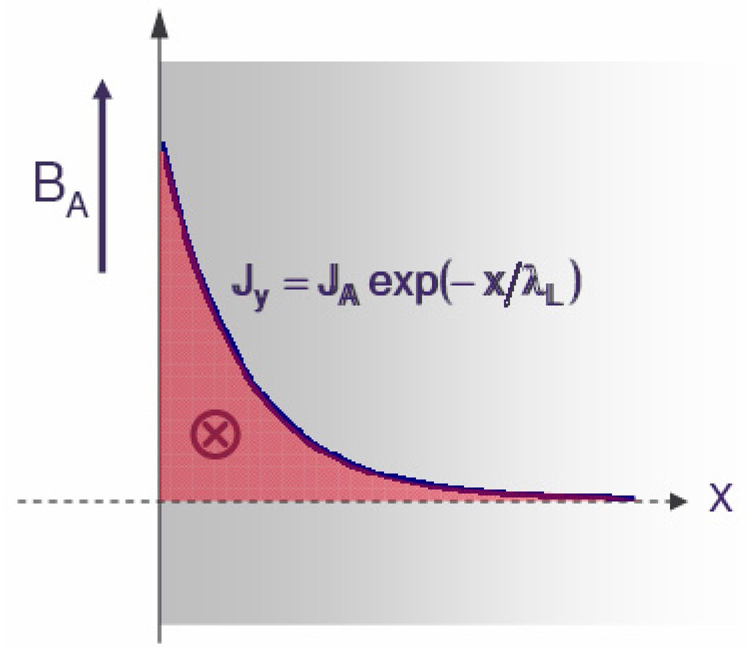

The magnetic field, and the current, decay exponentially over a distance λ (a few 10s of nm)

Model of F & H London (1935)

$$\lambda_L = \left[\frac{m}{\mu_0 n_s e^2}\right]^{\frac{1}{2}}$$

From Gorter and Casimir two-fluid model

$$n_s \propto \left[1 - \left(\frac{T}{T_C}\right)^4\right]$$

$$\lambda_L(T) = \lambda_L(0)\frac{1}{\left[1 - \left(\frac{T}{T_C}\right)^4\right]^{\frac{1}{2}}}$$

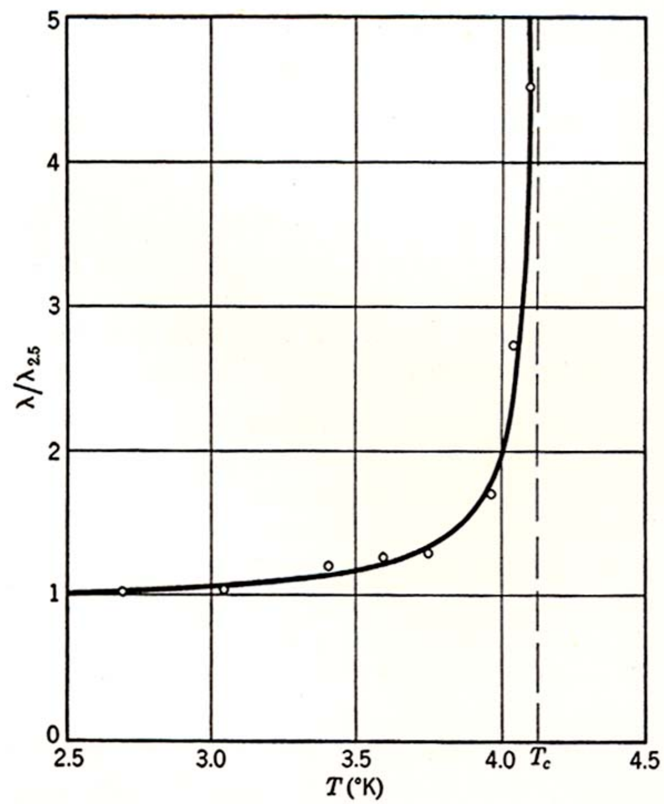

Fig. 21. Penetration depth as a function of temperature. (After Shoenberg, *Nature*, **43**, 433, 1939.)

Model of F & H London (1935)

London Equation: $\lambda^2 \nabla \times \vec{J}_s = -\dfrac{\vec{B}}{\mu_0} = -\vec{H}$

$$\nabla \times \vec{A} = \vec{H}$$

choose $\nabla \bullet \vec{A} = 0,$ $A_n = 0$ on sample surface (London gauge)

$$\boxed{\vec{J}_s = -\frac{1}{\lambda^2}\vec{A}}$$

Note: Local relationship between $\vec{J}_s$ and $\vec{A}$

Penetration Depth in Thin Films

Very thin films

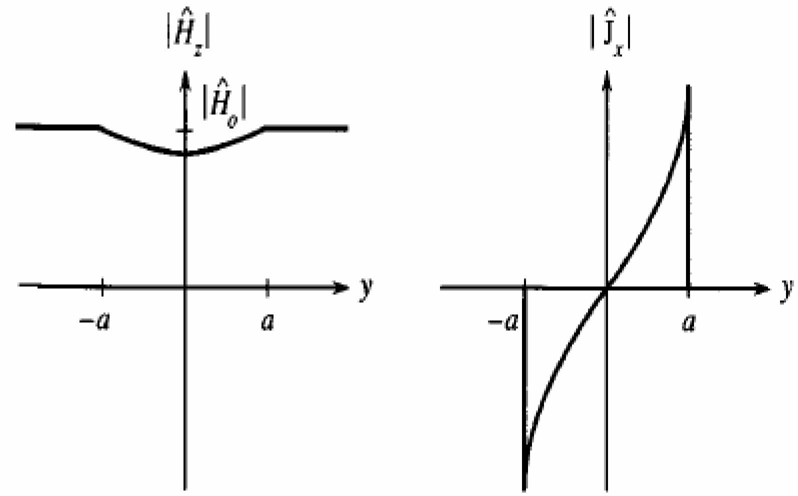

Very thick films

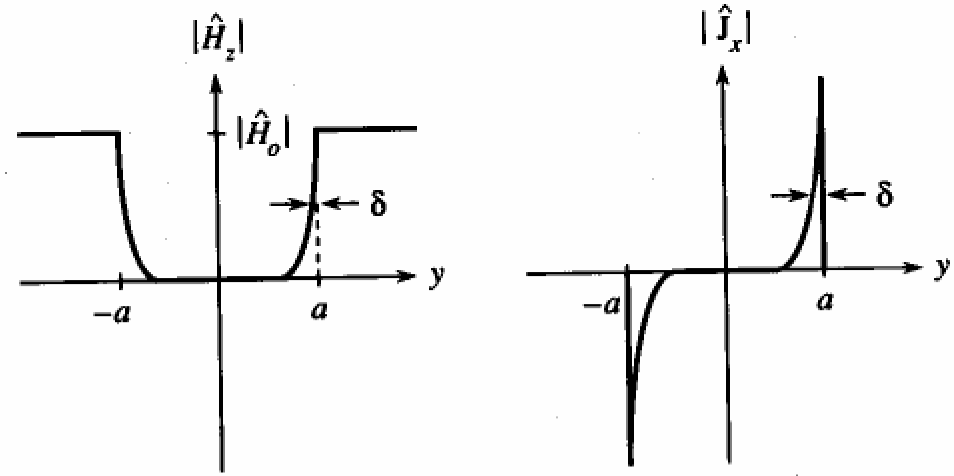

Quantum Mechanical Basis for London Equation

$$\vec{J}(r) = \sum_n \int \left\{ \frac{e\hbar}{2mi} \left[\psi^* \nabla_n \psi - \psi \nabla_n \psi^* \right] - \frac{e^2}{mc} \vec{A}(\vec{r}_n) \psi^* \psi \right\} \delta(r - r_n)\, dr_1 - dr_n$$

In zero field $\vec{A} = 0 \quad \vec{J}(r) = 0, \qquad \psi = \psi_0$

Assume ψ is "rigid", ie the field has no effect on wave function

$$\vec{J}(r) = -\frac{\rho(r) e^2}{m\, e} \vec{A}(r)$$

$$\rho(r) = n$$

Pippard's Extension of London's Model

Observations:

-Penetration depth increased with reduced mean free path

- H_c and T_c did not change

- Need for a positive surface energy over 10^{-4} cm to explain existence of normal and superconducting phase in intermediate state

Non-local modification of London equation

Local: $$\vec{J} = -\frac{1}{c\lambda}\vec{A}$$

Non local: $$\vec{J}(r) = -\frac{3\sigma}{4\pi\xi_0\lambda c}\int \frac{\vec{R}\left[\vec{R}\bullet\vec{A}(r')\right]e^{-\frac{R}{\xi}}}{R^4}\,d\upsilon$$

$$\frac{1}{\xi} = \frac{1}{\xi_0} + \frac{1}{\ell}$$

London and Pippard Kernels

Apply Fourier transform to relationship between

$J(r)$ and $A(r)$: $$J(k) = -\frac{c}{4\pi} K(k)\; A(k)$$

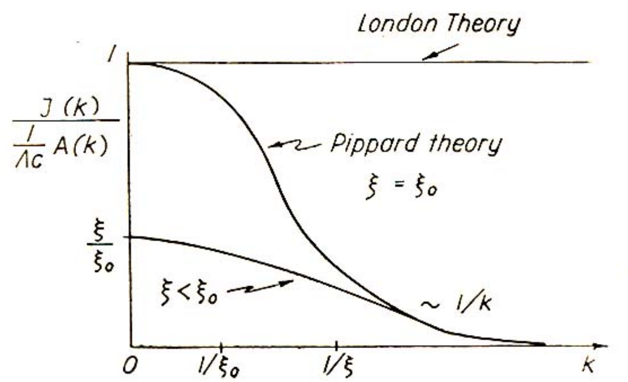

Fig. 1. Comparison of supercurrent response to vector potential in London and Pippard theories (schematic).

Effective penetration depth

Specular: $$\lambda_{eff} = \frac{2}{\pi}\int_o^\infty \frac{dk}{K(k)+k^2}$$

Diffuse: $$\lambda_{eff} = \frac{\pi}{\int_o^\infty \ln\left[1+\frac{K(k)}{k^2}\right]dk}$$

London Electrodynamics

Linear London equations

$$\frac{\partial \vec{J}_s}{\partial t} = -\frac{\vec{E}}{\lambda^2 \mu_0} \qquad \nabla^2 \vec{H} - \frac{1}{\lambda^2}\vec{H} = 0$$

together with Maxwell equations

$$\nabla \times \vec{H} = \vec{J}_s \qquad \nabla \times \vec{E} = -\mu_0 \frac{\partial \vec{H}}{\partial t}$$

describe the electrodynamics of superconductors at all T if:

- **The superfluid density n_s is spatially uniform**
- **The current density J_s is small**

Ginzburg-Landau Theory

- Many important phenomena in superconductivity occur because n_s is not uniform
  - Interfaces between normal and superconductors
  - Trapped flux
  - Intermediate state

- London model does not provide an explanation for the surface energy (which can be positive or negative)

- GL is a generalization of the London model but it still retain the local approximation of the electrodynamics

Ginzburg-Landau Theory

- Ginzburg-Landau theory is a particular case of Landau's theory of second order phase transition
- Formulated in 1950, before BCS
- Masterpiece of physical intuition
- Grounded in thermodynamics
- Even after BCS it still is very fruitful in analyzing the behavior of superconductors and is still one of the most widely used theory of superconductivity

Ginzburg-Landau Theory

- Theory of second order phase transition is based on an order parameter which is zero above the transition temperature and non-zero below
- For superconductors, GL use a complex order parameter $\Psi(r)$ such that $|\Psi(r)|^2$ represents the density of superelectrons
- The Ginzburg-Landau theory is valid close to T_c

Ginzburg-Landau Equation for Free Energy

- **Assume that Ψ(r) is small and varies slowly in space**
- **Expand the free energy in powers of Ψ(r) and its derivative**

$$f = f_{n0} + \alpha|\psi|^2 + \frac{\beta}{2}|\psi|^4 + \frac{1}{2m^*}\left|\left(\frac{\hbar}{i}\nabla - \frac{e^*}{c}\mathbf{A}\right)\psi\right|^2 + \frac{h^2}{8\pi}$$

Field-Free Uniform Case

$$f - f_{n0} = \alpha|\psi|^2 + \frac{\beta}{2}|\psi|^4$$

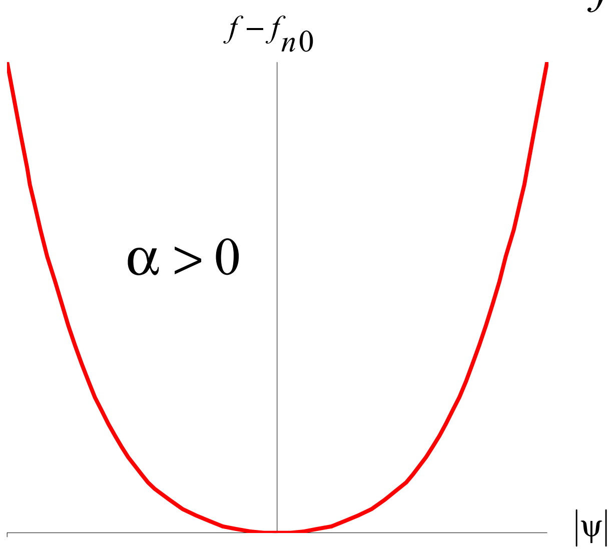

$$|\psi_\infty|^2 = -\frac{\alpha}{\beta}$$

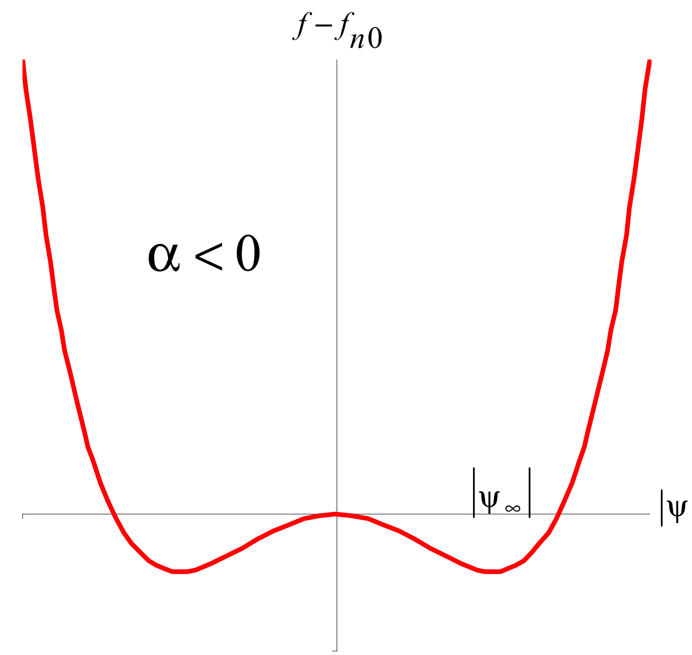

Near T_c we must have $\beta > 0$ $\alpha(t) = \alpha'(t-1)$

At the minimum $f - f_{n0} = -\frac{H_c^2}{8\pi} = -\frac{\alpha^2}{2\beta} \Rightarrow |\psi|^2$ and $H_c \propto (1-t)$

Field-Free Uniform Case

$$f - f_{n0} = \alpha|\psi|^2 + \frac{\beta}{2}|\psi|^4 \qquad\qquad |\psi_\infty|^2 = -\frac{\alpha}{\beta}$$

$$\beta > 0 \qquad \alpha(t) = \alpha'(t-1) \qquad \Rightarrow |\psi_\infty|^2 \propto (1-t)$$

It is consistent with correlating $|\Psi(r)|^2$ with the density of superelectrons

$$n_s \propto \lambda^{-2} \propto (1-t) \text{ near } T_c$$

At the minimum $$f - f_{n0} = -\frac{\alpha^2}{2\beta} = -\frac{H_c^2}{8\pi} \quad (\text{definition of } H_c)$$

$$\Rightarrow H_c \propto (1-t)$$

which is consistent with $H_c = H_{c0}\left(1-t^2\right)$

Field-Free Uniform Case

Identify the order parameter with the density of superelectrons

$$n_s = |\Psi|^2 \sim \frac{1}{\lambda_L^2(T)} \qquad \Rightarrow \quad \frac{\lambda_L^2(0)}{\lambda_L^2(T)} = \frac{|\Psi(T)|^2}{|\Psi(0)|^2} = -\frac{1}{n}\frac{\alpha(T)}{\beta}$$

since $\dfrac{1}{2}\dfrac{\alpha^2(T)}{\beta} = \dfrac{H_c^2(T)}{8\pi}$

$$n\alpha(T) = -\frac{H_c^2(T)}{4\pi}\frac{\lambda_L^2(T)}{\lambda_L^2(0)} \quad \text{and} \quad n^2\beta = \frac{H_c^2(T)}{4\pi}\frac{\lambda_L^4(T)}{\lambda_L^4(0)}$$

Field-Free Nonuniform Case

Equation of motion in the absence of electromagnetic field

$$-\frac{1}{2m^*}\nabla^2\psi + \alpha(T)\psi + \beta\left|\psi\right|^2\psi = 0$$

Look at solutions close to the constant one

$$\psi = \psi_\infty + \delta \quad \text{where} \quad \left|\psi_\infty\right|^2 = -\frac{\alpha(T)}{\beta}$$

To first order: $$\frac{1}{4m^*\left|\alpha(T)\right|}\nabla^2\delta - \delta = 0$$

Which leads to $$\delta \approx e^{-\sqrt{2}r/\xi(T)}$$

Field-Free Nonuniform Case

$$\delta \approx e^{-\sqrt{2}r/\xi(T)} \quad \text{where} \quad \xi(T) = \frac{1}{\sqrt{2m^*|\alpha(T)|}} = \sqrt{\frac{2\pi n}{m^* H_c^2(T)}} \frac{\lambda_L(0)}{\lambda_L(T)}$$

is the Ginzburg-Landau coherence length.

It is different from, but related to, the Pippard coherence length.

$$\xi(T) \simeq \frac{\xi_0}{\left(1-t^2\right)^{1/2}}$$

GL parameter:

$$\kappa(T) = \frac{\lambda_L(T)}{\xi(T)}$$

Both $\lambda_L(T)$ and $\xi(T)$ diverge as $T \to T_c$ but their ratio remains finite

$\kappa(T)$ is almost constant over the whole temperature range

2 Fundamental Lengths

London penetration depth: length over which magnetic field decay

$$\lambda_L(T) = \left(\frac{m^* \beta}{2e^2 \alpha'}\right)^{1/2} \sqrt{\frac{T_c}{T_c - T}}$$

Coherence length: scale of spatial variation of the order parameter (superconducting electron density)

$$\xi(T) = \left(\frac{\hbar^2}{4m^* \alpha'}\right)^{1/2} \sqrt{\frac{T_c}{T_c - T}}$$

The critical field is directly related to those 2 parameters

$$H_c(T) = \frac{\phi_0}{2\sqrt{2}\,\xi(T)\,\lambda_L(T)}$$

Surface Energy

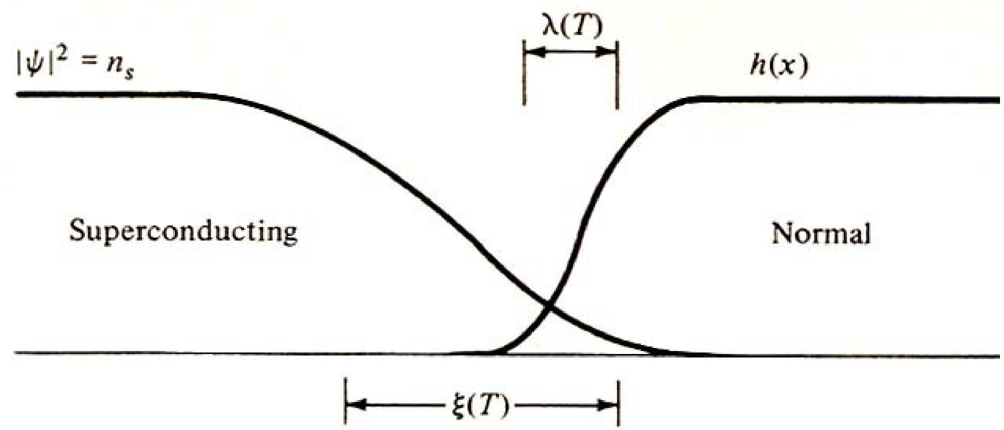

$$\sigma \simeq \frac{1}{8\pi}\left[H_c^2\xi - H^2\lambda\right]$$

$\frac{H^2\lambda}{8\pi}$: Energy that can be gained by letting the fields penetrate

$\frac{H_c^2\xi}{8\pi}$: Energy lost by "damaging" superconductor

Surface Energy

$$\sigma \simeq \frac{1}{8\pi}\left[H_c^2\xi - H^2\lambda\right]$$

Interface is stable if σ>0

If $\xi >> \lambda$ σ>0

Superconducting up to H_c where superconductivity is destroyed globally

If λ >>ξ σ<0 for $H^2 > H_c^2 \frac{\xi}{\lambda}$

Advantageous to create small areas of normal state with large area to volume ratio

$\rightarrow$ quantized fluxoids

More exact calculation (from Ginzburg-Landau):

$\kappa = \frac{\lambda}{\xi} < \frac{1}{\sqrt{2}}$: Type I

$\kappa = \frac{\lambda}{\xi} > \frac{1}{\sqrt{2}}$: Type II

Magnetization Curves

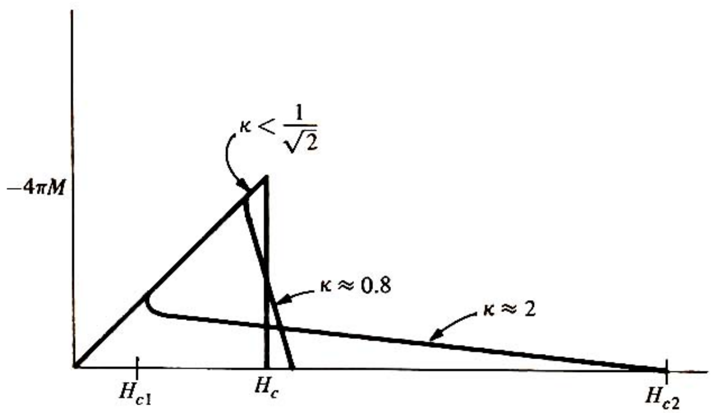

FIGURE 5-2
Comparison of magnetization curves for three superconductors with the same value of thermodynamic critical field H_c, but different values of κ. For $\kappa < 1/\sqrt{2}$, the superconductor is of type I and exhibits a first-order transition at H_c. For $\kappa > 1/\sqrt{2}$, the superconductor is type II and shows second-order transitions at H_{c1} and H_{c2} (for clarity, marked only for the highest κ case). In all cases, the area under the curve is the condensation energy $H_c^2/8\pi$.

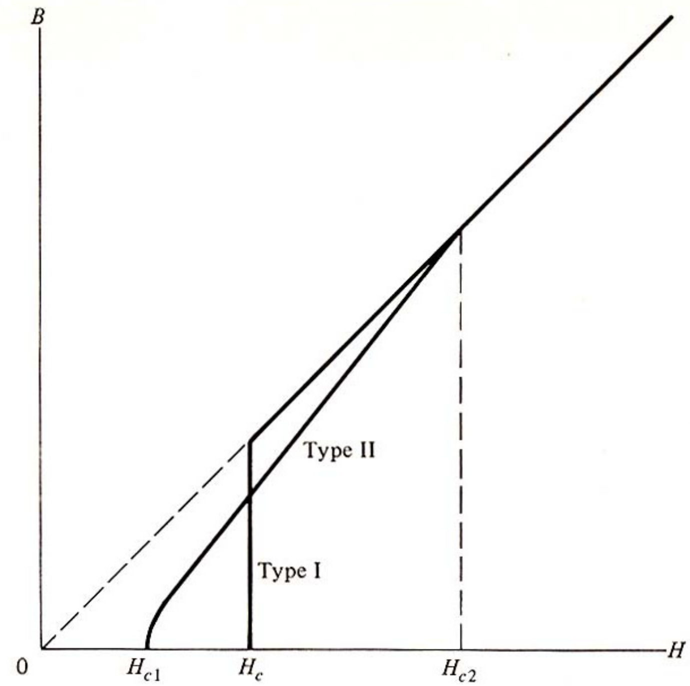

FIGURE 1-5
Comparison of flux penetration behavior of type I and type II superconductors with the same thermodynamic critical field H_c. $H_{c2} = \sqrt{2}\kappa H_c$. The ratio of B/H_{c2} from this plot also gives the approximate variation of R/R_n, where R is the electrical resistance for the case of negligible pinning, and R_n is the normal-state resistance.

Intermediate State

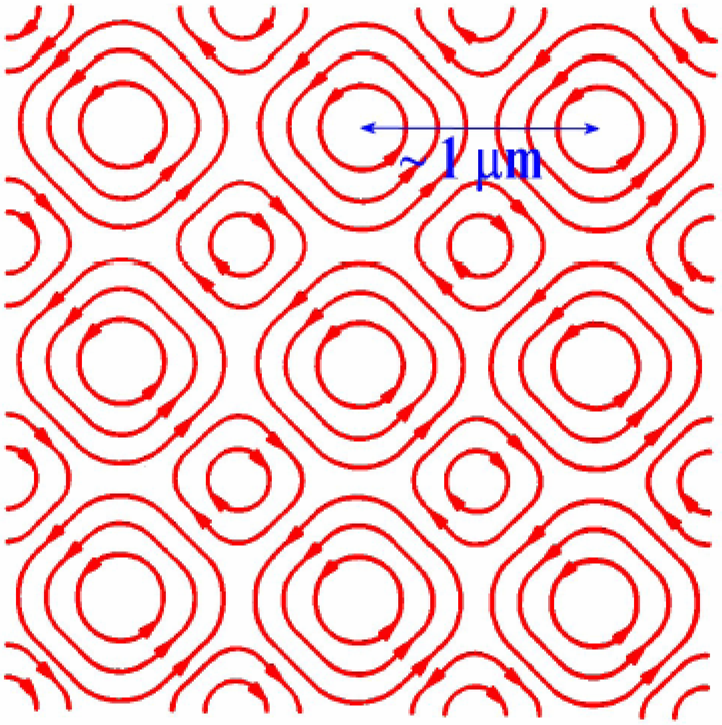

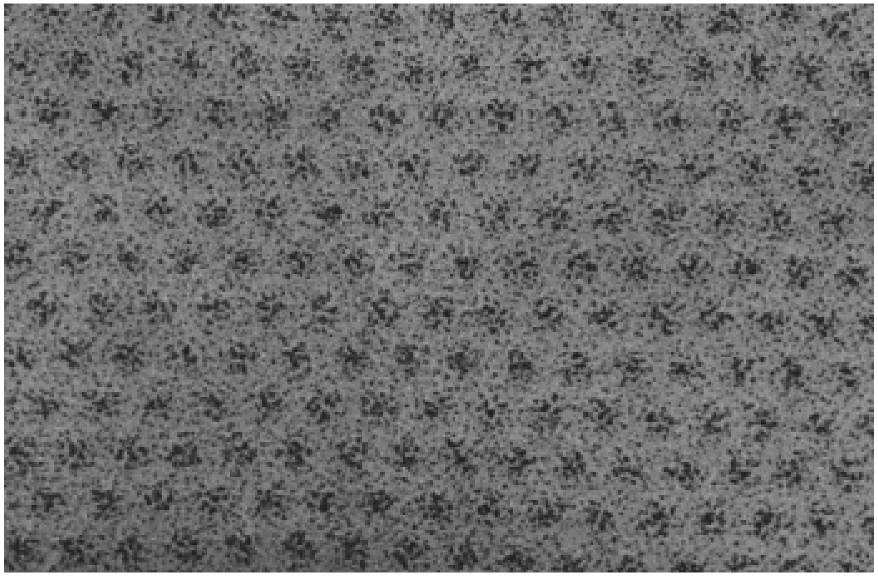

Vortex lines in $Pb_{.98}In_{.02}$

At the center of each vortex is a normal region of flux h/2e

Critical Fields

Even though it is more energetically favorable for a type I superconductor to revert to the normal state at H_c, the surface energy is still positive up to a superheating field $H_{sh}>H_c \rightarrow$ metastable superheating region in which the material may remain superconducting for short times.

Type I

H_c Thermodynamic critical field

$H_{sh} \simeq \frac{H_c}{\sqrt{\kappa}}$ Superheating critical field

Field at which surface energy is

Type II

H_c Thermodynamic critical field

$$H_{c2} = \sqrt{2}\ \kappa\ H_c$$

$$H_{c1} \simeq \frac{H_c^2}{H_{c2}}$$

$$\simeq \frac{1}{2\kappa}(\ln\kappa + .008)H_c \qquad (\text{for } \kappa \gg 1)$$

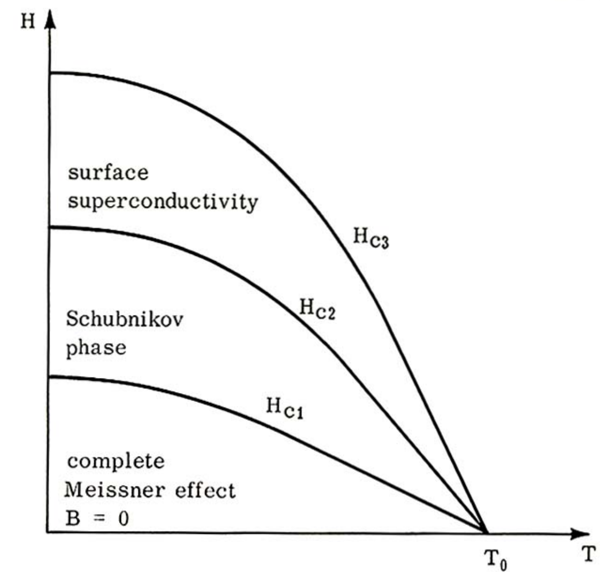

Figure 3-1
Phase diagram for a long cylinder of a Type II superconductor.

Superheating Field

Ginsburg-Landau:

$$H_{sh} \sim \frac{0.9 H_c}{\sqrt{\kappa}} \quad \text{for } \kappa << 1$$

$$\sim \quad 1.2 \ H_c \quad \text{for } \kappa \sim 1$$

$$\sim \quad 0.75 \ H_c \quad \text{for } \kappa >> 1$$

The exact nature of the rf critical field of superconductors is still an open question

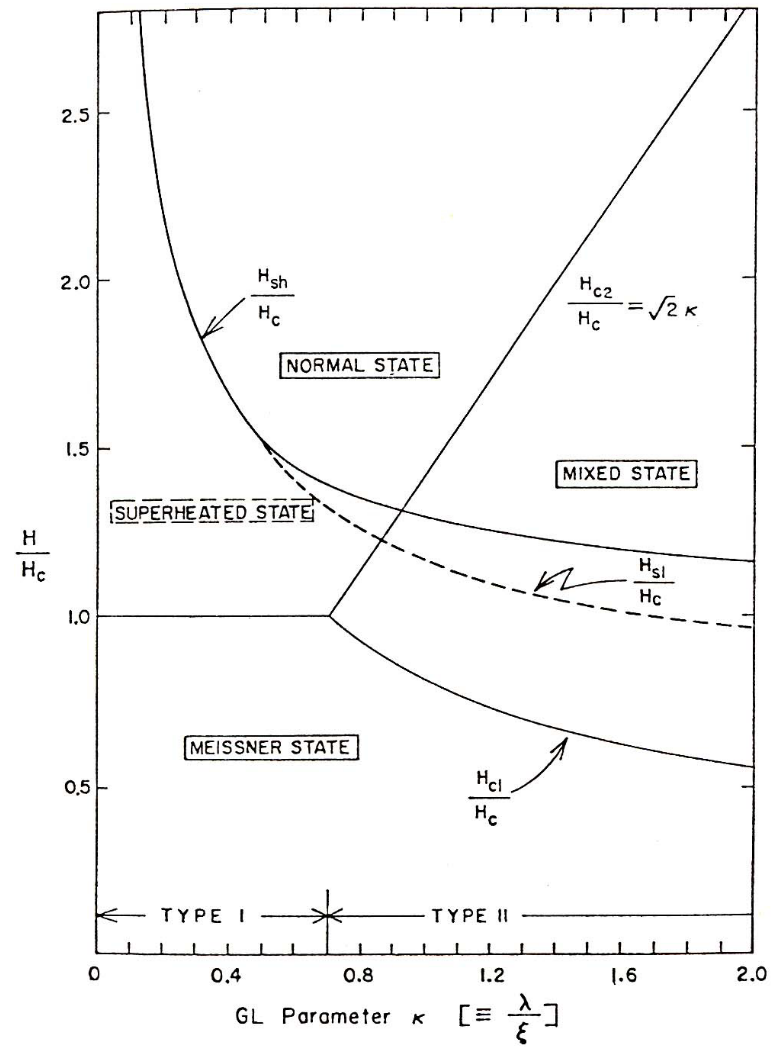

Fig. 13: Phase diagram of superconductors[42] in the transition regime of type I and II. The normalized critical fields are shown as a function of $\varkappa$.

Material Parameters for Some Superconductors

Superconductor	λ_L (0) (nm)	ξ_0 (nm)	κ	$2\Delta(0)/kT_c$	T_c(K)
Al	16	1500	0.011	3.40	1.18
In	25	400	0.062	3.50	3.3
Sn	28	300	0.093	3.55	3.7
Pb	28	110	0.255	4.10	7.2
Nb	32	39	0.82	3.5-3.85	8.95-9.2
Ta	35	93	0.38	3.55	4.46
Nb_3Sn	50	6	8.3	4.4	18
NbN	50	6	8.3	4.3	≤ 17
$Yba_2Cu_3o_x$	140	1.5	93	4.5	90

BCS

- What needed to be explained and what were the clues?
  - Energy gap (exponential dependence of specific heat
  - Isotope effect (the lattice is involved)
  - Meissner effect

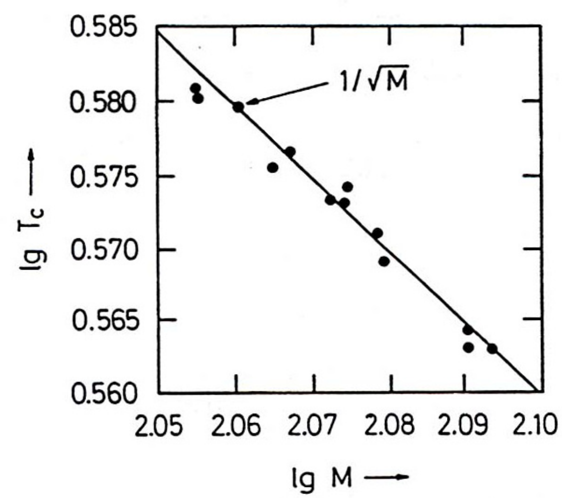

Figure 26: The critical temperature of various tin isotopes.

Cooper Pairs

Assumption: Phonon-mediated attraction between electron of equal and opposite momenta located within $\hbar\omega_D$ of Fermi surface

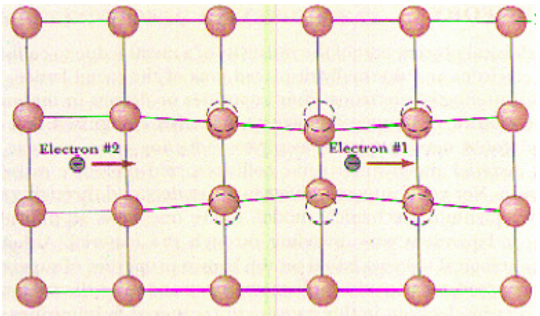

Moving electron distorts lattice and leaves behind a trail of positive charge that attracts another electron moving in opposite direction

Fermi ground state is unstable

Electron pairs can form bound states of lower energy

Bose condensation of overlapping Cooper pairs into a coherent Superconducting state

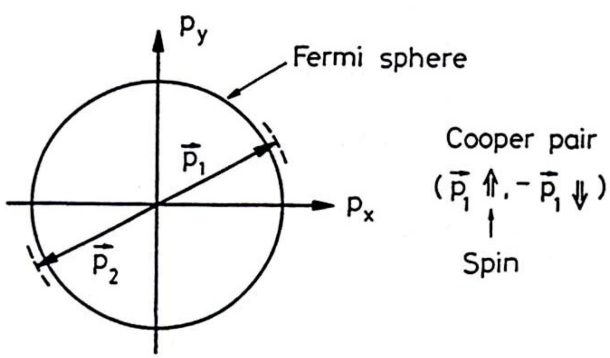

Figure 20: A pair of electrons of opposite momenta added to the full Fermi sphere.

Cooper Pairs

One electron moving through the lattice attracts the positive ions.

Because of their inertia the maximum displacement will take place

$d \approx v_F \dfrac{2\pi}{\omega_D} \approx 100 - 1000\,\mathrm{nm}$ behind.

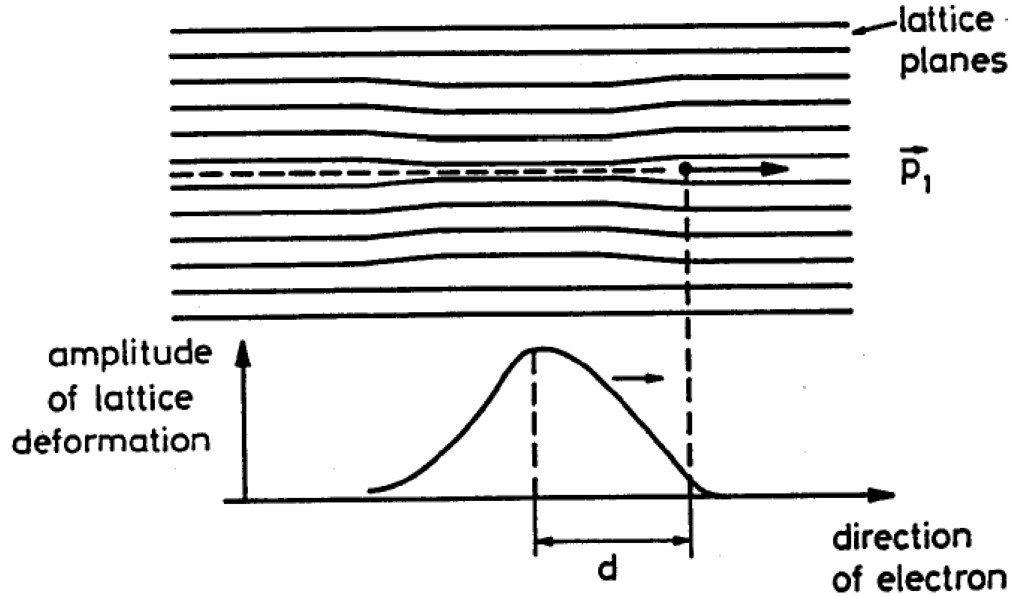

BCS

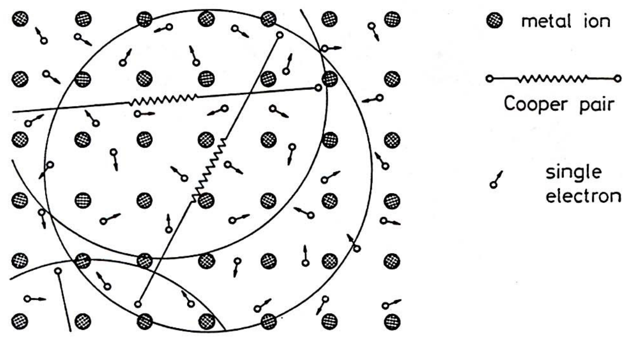

Figure 22: Cooper pairs and single electrons in the crystal lattice of a superconductor. (After Essmann and Träuble [12]).

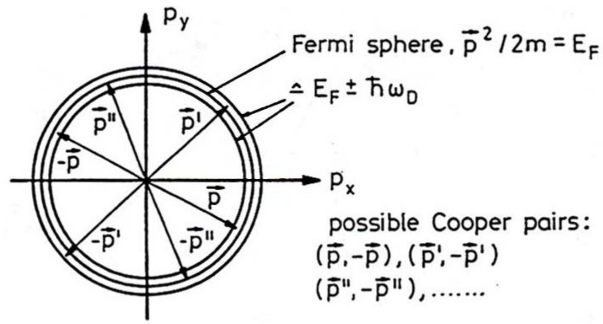

Figure 23: Various Cooper pairs $(\vec{p}, -\vec{p})$, $(\vec{p}\,', -\vec{p}\,')$, $(\vec{p}\,'', -\vec{p}\,'')$, ... in momentum space.

The size of the Cooper pairs is much larger than their spacing

They form a coherent state

BCS and BEC

BCS	BEC
weak coupling	strong coupling
large pair size **k**-space pairing	small pair size **r**-space pairing
strongly overlapping Cooper pairs	ideal gas of preformed pairs

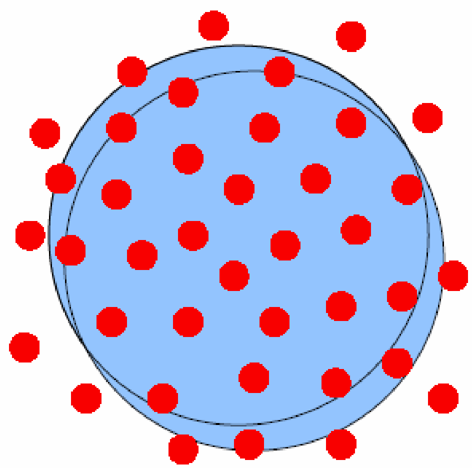

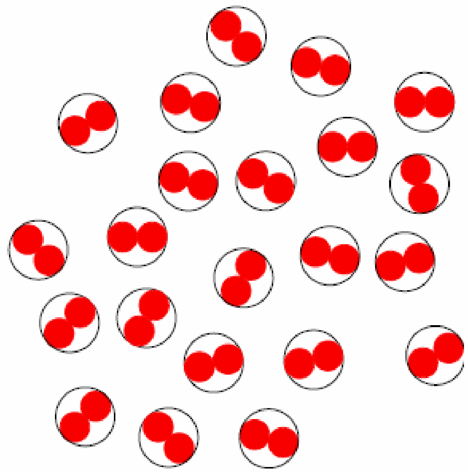

BCS Theory

$|0\rangle_q, |1\rangle_q$:states where pairs $(\vec{q},\text{-}\vec{q})$ are unoccupied, occupied

a_q, b_q : probabilites that pair $(\vec{q},\text{-}\vec{q})$ is unoccupied, occupied

BCS ground state

$$|\Psi\rangle = \prod_{\vec{q}} \left(a_q |0\rangle_q + b_q |1\rangle_q \right)$$

Assume interaction between pairs $\vec{q}$ and $\vec{k}$

$$V_{qk} = -V \text{ if } |\xi_q| \le \hbar\omega_D \text{ and } |\xi_k| \le \hbar\omega_D$$
$$= 0 \text{ otherwise}$$

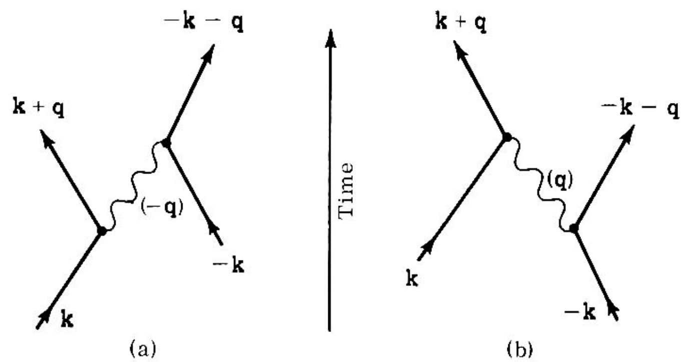

Figure 4-1
Electron-electron interaction via phonons. In process (a) the electron **k** emits a phonon of wave-vector −**q**. The phonon is absorbed later by the second electron. In process (b) the second electron in state (−**k**) emits a phonon **q**, subsequently absorbed by the first electron.

BCS

- Hamiltonian

$$\mathscr{H} = \sum_{k} \varepsilon_k n_k + \sum_{qk} V_{qk} c_q^* c_{-q}^* c_k c_{-k}$$

c_k destroys an electron of momentum k

c_q^* creates an electron of momentum k

$n_k = c_k^* c_k$ number of electrons of momentum k

- Ground state wave function

$$\left|\Psi\right\rangle = \prod_{\vec{q}} \left(a_q + b_q c_q^* c_{-q}^*\right)\left|\phi_0\right\rangle$$

BCS

- The BCS model is an extremely simplified model of reality
  - The Coulomb interaction between single electrons is ignored
  - Only the term representing the scattering of pairs is retained
  - The interaction term is assumed to be constant over a thin layer at the Fermi surface and 0 everywhere else
  - The Fermi surface is assumed to be spherical

- Nevertheless, the BCS results (which include only a very few adjustable parameters) are amazingly close to the real world

BCS

Is there a state of lower energy than the normal state?

$$a_q = 0,\ b_q = 1 \qquad \text{for} \quad \xi_q < 0$$

$$a_q = 1,\ b_q = 0 \qquad \text{for} \quad \xi_q > 0$$

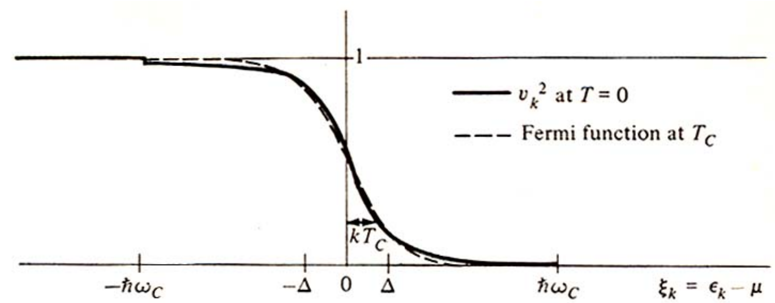

FIGURE 2-1
Plot of BCS occupation fraction v_k^2 vs. electron energy measured from the chemical potential (Fermi energy). To make the cutoffs at $\pm\hbar\omega_c$ visible, the plot has been made for a strong-coupling superconductor with $N(0)V = 0.43$. For comparison, the Fermi function for the normal state at T_c is also shown on the same scale, using the BCS relation $\Delta(0) = 1.76kT_c$.

yes: $$2b_q^2 = 1 - \frac{\xi_q}{\sqrt{\xi_q^2 + \Delta_0^2}}$$

where

$$\Delta_0 = \frac{\hbar\omega_D}{\sinh\left[\dfrac{1}{\rho(0)V}\right]} \simeq 2\hbar\omega_D\ e^{-\frac{1}{\rho(0)V}}$$

BCS

Critical temperature

$$kT_c = \quad 1.14\,\hbar\omega_D \quad \exp\left[-\frac{1}{VN(E_F)}\right]$$

$$\Delta(0) = \quad 1.76\;kT_c$$

element	Sn	In	Tl	Ta	Nb	Hg	Pb
$\Delta(0)/k_B T_c$	1.75	1.8	1.8	1.75	1.75	2.3	2.15

Coherence length (the size of the Cooper pairs)

$$\xi_0 = .18\frac{\hbar\upsilon_F}{kT_c}$$

BCS Condensation Energy

Condensation energy: $$E_s - E_n = -\frac{\rho(0) V \Delta_0^2}{2}$$

$$\simeq -N\Delta_0 \left(\frac{\Delta_0}{\varepsilon_F}\right) = \frac{H_0^2}{8\pi}$$

$$\Delta_0 / k \simeq 10K$$

$$\varepsilon_F / k \simeq 10^4 K$$

BCS Energy Gap

At finite temperature:

Implicit equation for the temperature dependence of the gap:

$$\frac{1}{V\rho(0)} = \int_0^{\hbar\omega_D} \frac{\tanh\left[\left(\varepsilon^2+\Delta^2\right)^{1/2}/2kT\right]}{\left(\varepsilon^2+\Delta^2\right)^{1/2}} d\varepsilon$$

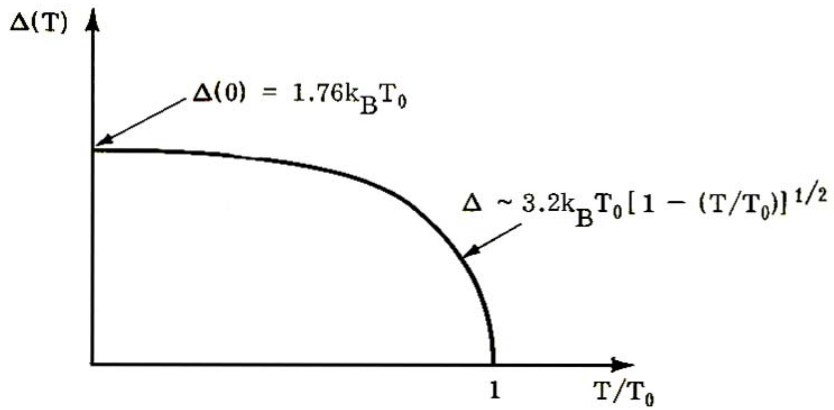

Figure 4-4
Variation of the order parameter Δ with temperature in the BCS approximation.

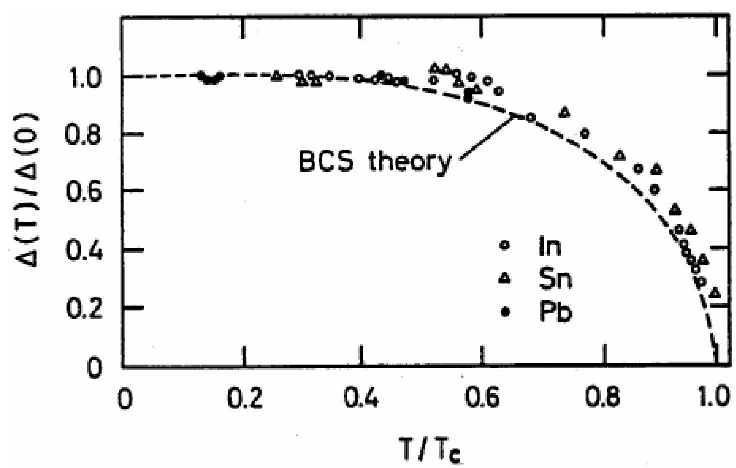

BCS Excited States

Energy of excited states:

$$\varepsilon_k = 2\sqrt{\xi_k^2 + \Delta_0^2}$$

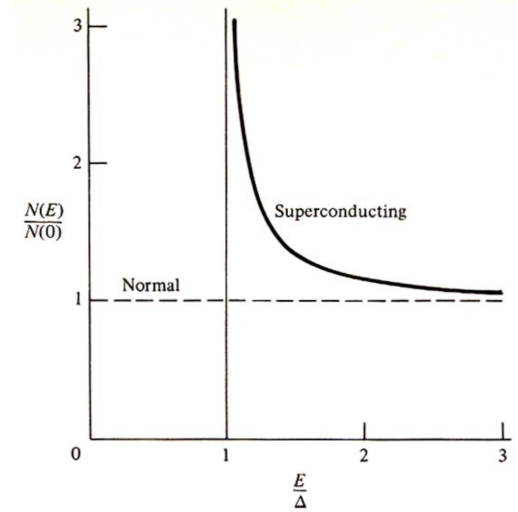

FIGURE 2-4
Density of states in superconducting compared to normal state. All **k** states whose energies fall in the gap in the normal metal are raised in energy above the gap in the superconducting state.

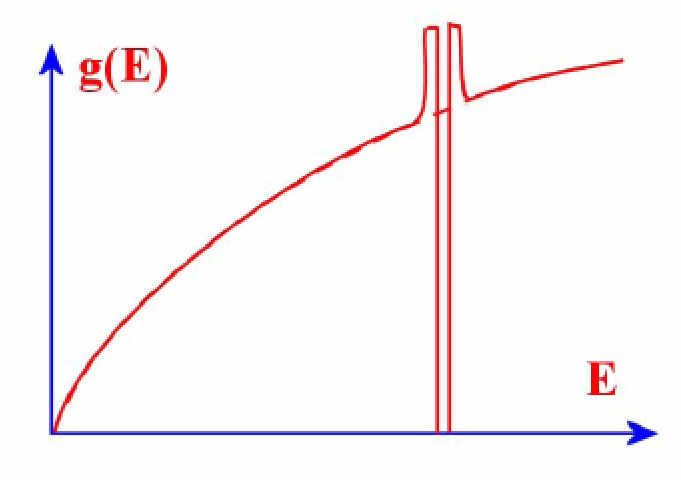

BCS Heat Capacity

Heat capacity

$$C_{es} \simeq \quad \exp\left(-\frac{\Delta}{kT}\right) \quad \text{for} \quad T < \frac{T_c}{10}$$

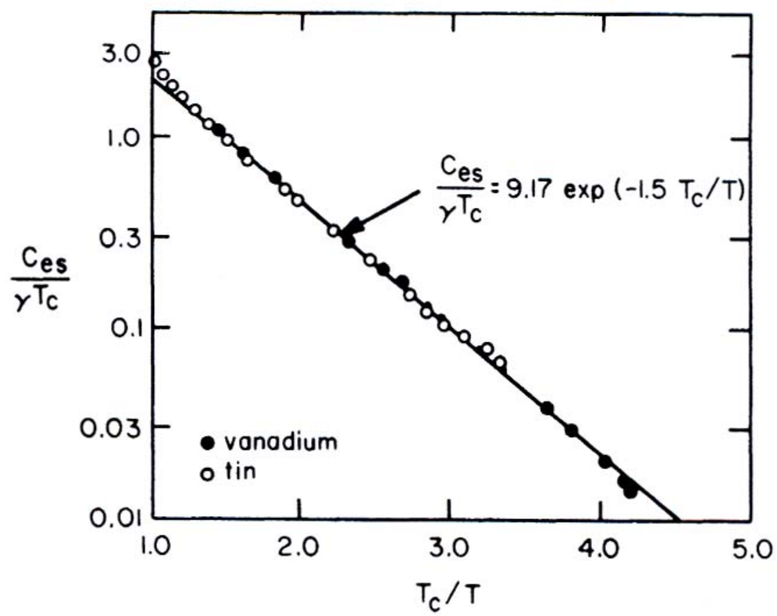

Fig. 22. Reduced electronic specific heat in superconducting vanadium and tin. [From Biondi et al., (*150*).]

Electrodynamics and Surface Impedance in BCS Model

$$H_0\phi + H_{ex}\ \phi = i\hbar\frac{\partial\phi}{\partial t}$$

$$H_{ex} = \frac{e}{mc}\sum A(r_i,t)\,p_i$$

H_{ex} is treated as a small perturbation

$$H_{rf} << H_c$$

There is, at present, no model for superconducting surface resistance at high rf field

$$J \propto \int \frac{R[R\cdot A]\,I(\omega,R,T)\,e^{-\frac{R}{l}}}{R^4}\,dr$$

similar to Pippard's model

$$J(k) = -\frac{c}{4\pi}K(k)\,A(k)$$

$K(0)\neq 0:$ Meissner effect

Penetration Depth

$$\lambda = \frac{2}{\pi} \int \frac{dk}{K(k) + k^2} dk \qquad \text{(specular)}$$

Represented accurately by $\lambda \sim \dfrac{1}{\sqrt{1 - \left(\dfrac{T_c}{T}\right)^4}}$ near T_c

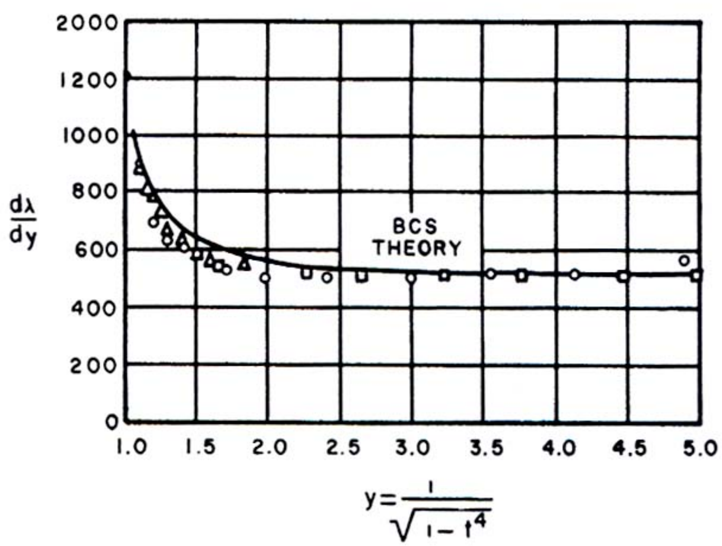

Fig. 30. Temperature dependence of $d\lambda/dy$ for tin obtained by Schawlow and Devlin (*207*) compared with the theoretical curve obtained from the BCS theory.

Surface Resistance

Temperature dependence

–close to T_c : dominated by change in $\lambda(t)$ $\dfrac{t^4}{\left(1-t^2\right)^{3/2}}$

–for $T < \dfrac{T_c}{2}$: dominated by density of excited states $\sim e^{-\Delta/kT}$

$$R_s \sim \frac{A}{T}\omega^2 \exp\left(-\frac{\Delta}{kT}\right)$$

Frequency dependence

ω^2 is a good approximation

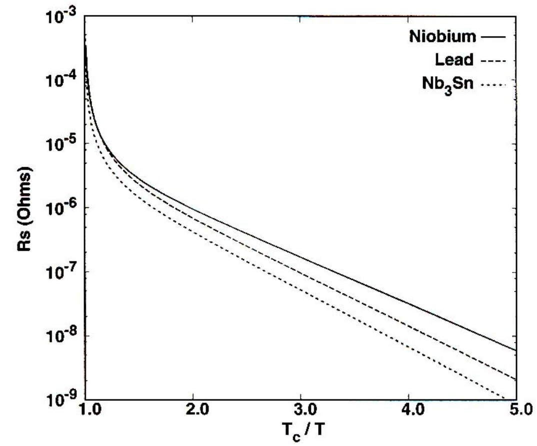

Figure 4.5: Theoretical surface resistance at 1.5 GHz of lead, niobium and Nb_3Sn as calculated from program [94]. The values given in Table 4.1 were used for the material parameters.

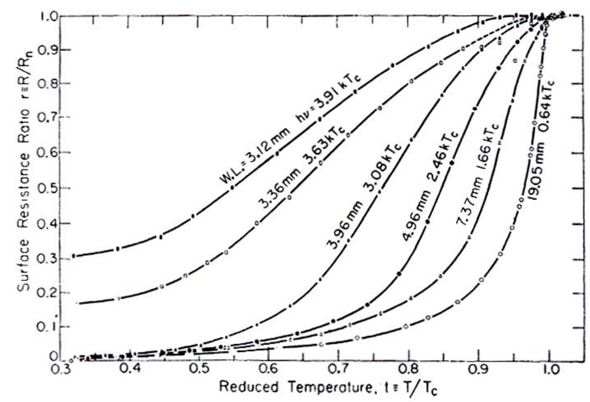

Fig. 1. Measured values of the surface resistance ratio r of superconducting aluminum as a function of the reduced temperature t at several representative wavelengths. The wavelengths and corresponding photon energies are indicated on the curves [After Biondi and Garfunkel (*15*).]

Surface Resistance

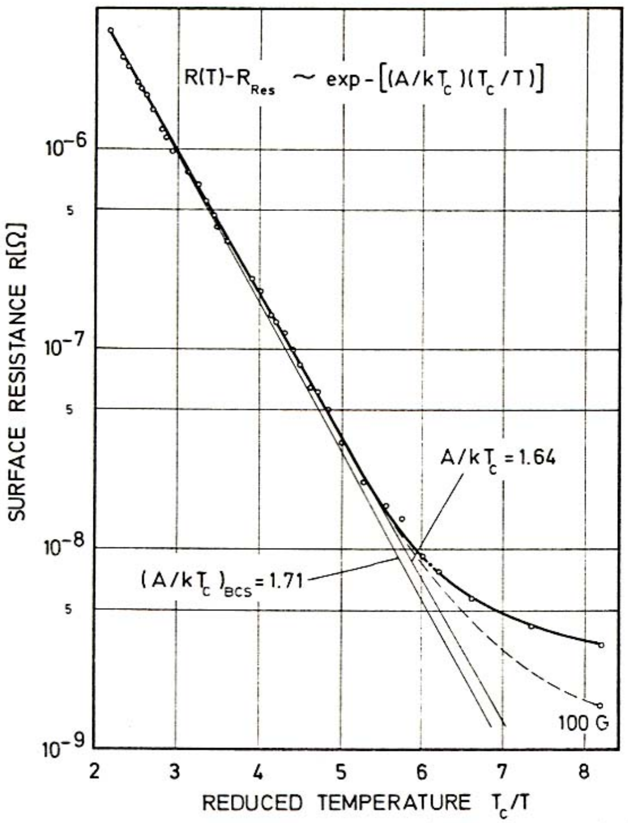

Fig. 2. Temperature dependence of surface resistance of niobium at 3.7 GHz measured in the TE_{011} mode at $H_{rf} \simeq 10$ G. The values computed with the BCS theory used the following material parameters:

$T_c = 9.25$ K; $\lambda_L(T=0, l=\infty) = 320$ Å;

$\Delta(0)/kT = 1.85$; $\xi_F(T=0, l=\infty) = 620$ Å; $l = 1000$ Å or 80 Å.

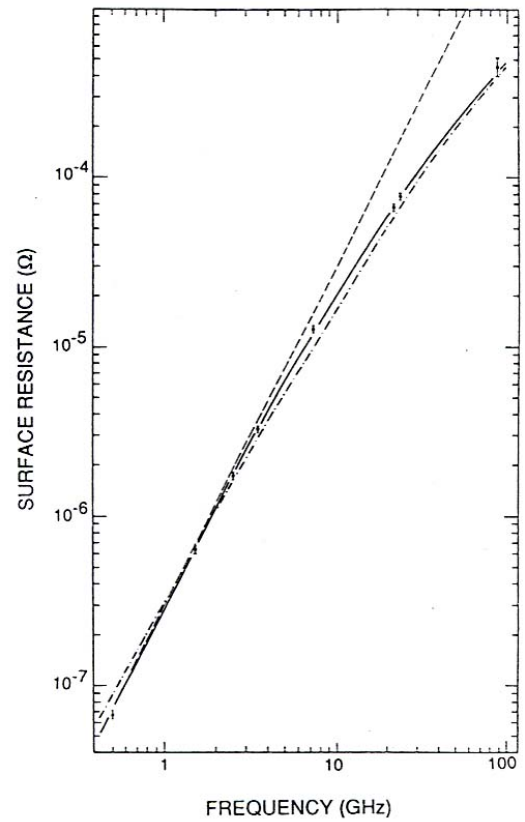

Fig. 5. The surface resistance of Nb at 4.2 K as a function of frequency [62,63]. Whereas the isotropic BCS surface resistance (– · – ·) resulted in $R \propto \omega^{1.8}$ around 1 GHz, the measurements fit better to ω^2 (– – –). The solid curve, which fits the data over the entire range, is a calculation based on the smearing of the BCS density-of-states singularity by the energy gap anisotropy in the presence of impurity scattering [61]. The authors thank G. Müller for providing this figure.